JACS
JOURNAL OF THE AMERICAN CHEMICAL SOCIETY
Article
pubs.acs.org/JACS

Membrane-Inspired Acidically Stable Dye-Sensitized Photocathode for Solar Fuel Production

Kevin A. Click,[†] Damian R. Beauchamp,[†] Zhongjie Huang,[†] Weilin Chen,[‡] and Yiying Wu*[,†]

[†]Department of Chemistry and Biochemistry, The Ohio State University, 100 West 18th Avenue, Columbus, Ohio 43210, United States

[‡]Key Laboratory of Polyoxometalate Science of Ministry of Education, Department of Chemistry, Northeast Normal University, Changchun, Jilin 130024, China

Supporting Information

ABSTRACT: Tandem dye-sensitized photoelectrochemical cells (DSPECs) for water splitting are a promising method for sustainable energy conversion but so far have been limited by their lack of aqueous stability and photocurrent mismatch between the cathode and anode. In nature, membrane-enabled subcellular compartmentation is a general approach to control local chemical environments in the cell. The hydrophobic tails of the lipid make the bilayer impermeable to ions and hydrophilic molecules. Herein we report the use of an organic donor−acceptor dye that prevents both dye desorption and semiconductor degradation by mimicking the hydrophobic/hydrophilic properties of lipid bilayer membranes. The dual-functional photosensitizer (denoted as BH4) allows for efficient light harvesting while also protecting the semiconductor surface from protons and water via its hydrophobic π linker. The protection afforded by this membrane-mimicking dye gives this system excellent stability in extremely acidic (pH 0) conditions. The acidic stability also allows for the use of cubane molybdenum-sulfide cluster as the hydrogen evolution reaction (HER) catalyst. This system produces a proton-reducing current of 183 ± 36 μA/cm^2 (0 V vs NHE with 300 W Xe lamp) for an unprecedented 16 h with no degradation. These results introduce a method for developing high-current, low-pH DSPECs and are a significant move toward practical dye-sensitized solar fuel production.

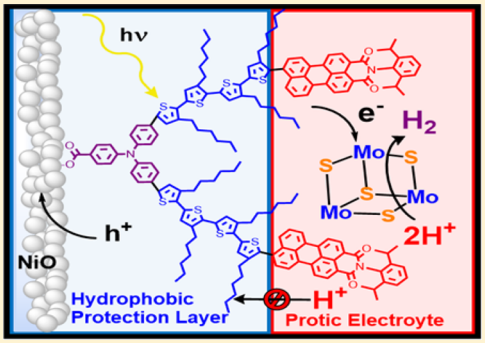

INTRODUCTION

Photocatalytic water splitting is an attractive solution for circumventing carbon dioxide producing fossil fuels as well as solar energy's intermittency. In particular, bias-free tandem water-splitting dye-sensitized photoelectrochemical cells (DSPECs)[1] have become an interesting, cost-effective, and promising method.[2] Tandem DSPECs have the advantage of rational molecular engineering of the sensitizer and the molecular catalyst. However, tandem DSPECs are limited by two main factors: mismatch between photocathode and photoanode current and photocurrent decay under long-term operation, especially in aqueous and acidic media.[3]

The photocurrent of a tandem DSPEC is limited by the lower current-producing electrode, which has been the photocathode.[3,4] Prior DSPEC research has focused on the photoanode exemplified by the pioneering works of Mallouk et al.,[5−7] Meyer et al.,[1,8,9] and others.[10−12] By contrast, research on dye-sensitized photocathodes for water splitting has been rare. The four devices examined to date[13−16] employed pH 7 buffer solutions and required an applied potential in order to produce an appreciable amount of current and hydrogen. Those photocathodes' current densities ranged from 10 to 20 μA/cm^2, which pales in comparison to the 1.7 mA/cm^2 so far achieved by the photoanode side.[11]

Photoelectrode stability for water splitting is another challenge. Ideally, low pH is favorable for improving kinetics of hydrogen production on the deficient photocathode side and allowing proton conducting membranes to be used to separate each half cell. It is also crucial that the photoanode side is stable in acidic conditions because local pH changes from the water oxidation reaction can cause dye degradation and desorption even at neutral pH, thus limiting the stability of the system.[3] However, typical devices' chronoamperometry (CA) experiments for water oxidation or reduction show only 10−100 s time frames that display noticeable photocurrent decay, even under neutral conditions.[17] In only a few exceptions, the current is maintained for a couple of hours.[14,18] Therefore, it is imperative to develop high-current and long-term aqueous photocathode stability for efficient tandem DSPECs.

Herein we report the first acidically stable p-type DSPEC. The key to the extended stability (16.6 h of illumination in pH 0) of our system lies within the molecular engineering of a dual-function organic photosensitizer, 4-(bis(4-(5‴-(2-(2,6-diisopropylphenyl)-1,3-dioxo-2,3-dihydro-1H-benzo[5,10]anthra[2,1,9-*def*]isoquinolin8-yl)-3,4′,4″,4‴-tetrahexyl-[2,2′:5′,2″:5″,2‴-quaterthiophen]-5-yl) phenyl)amino)benzoic acid (BH4).[19] BH4

Received: July 23, 2015
Published: January 8, 2016

DOI: 10.1021/jacs.5b07723
J. Am. Chem. Soc. 2016, 138, 1174−1179

is an organic push−double-pull dye (D−π−2A) that consists of a triphenylamine (TPA) donor moiety connected to two perylenemonoimide (PMI) acceptor groups by head-to-tail oligio-3-hexylthiophene-conjugated π-linker groups. This dye design mimics nature's thylakoid membranes of photosystems I and II.[20] The donor group layer, which contains the carboxylic acid functional group for loading onto NiO, is protected from the highly protic aqueous electrolyte (1 M HCl, pH 0) by the canopy of hydrophobic hexyl groups above it in the thiophene linkers. The PMI groups are located above the canopy of hydrophobic hexyl groups and act as the head layer whereby the aqueous electrolyte can interact. Upon photoexcitation, an electron can move from the donor (TPA) to the acceptors (PMI) whereby the charge-separated state is protected from charge recombination with NiO by the length of oligothiophene π linker, which is between the donor and acceptor.[21,22] The excited electron can interact with the electrolyte, which contains the catalyst, and the hole can be efficiently collected by NiO because it is protected from recombination with the electrolyte by the hydrophobic bulk of the hexyl groups (Figure 1).[23] BH4 is among the top-performing dyes for p-type DSSCs

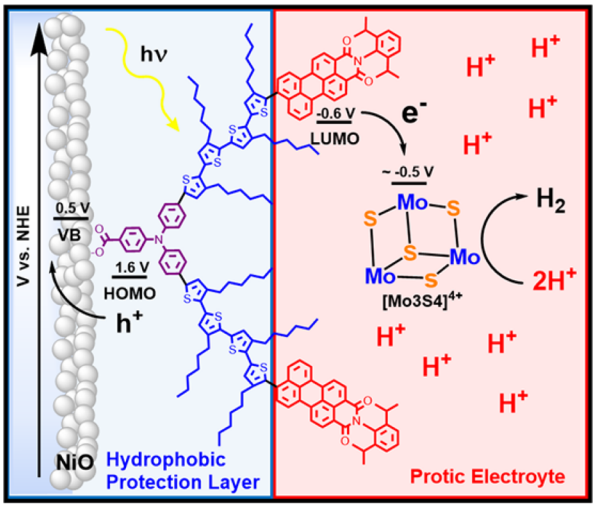

Figure 1. Molecular structure of BH4 and the schematic showing the energetics of the DSPEC.

and has one of the highest reported molar extinction coefficients (~100 000 M^{-1} cm^{-1} at 515 nm).[19] The high molar extinction coefficient allows for efficient light harvesting, producing average photocurrents of 183 ± 36 $\mu A/cm^2$ at an applied bias of 0 V vs NHE (All potentials from here are referenced vs NHE.) and as high as 300 $\mu A/cm^2$ at an applied bias of −0.2 V with 300 W Xe lamp illumination. This photocathode is the first to obtain currents as high as those obtained for the photoanode variants, allowing for more efficient tandem cells to be developed.[17]

Acidically stable and active HER catalysts are another crucial component of high-performance p-DSPECs. The aforementioned p-type systems have mainly used cobaloxime catalysts.[14,16] The cobaloxime catalyst was not chosen as an HER catalyst in this study because strong acid hydrolyzes the oximato functionality and uncoordinates the cobalt cation. The cobaloxime catalyst is also unsuitable because of its low solubility in water.[24] Instead, a cubane molybdenum sulfide cluster, $[Mo_3S_4]^{4+}$, was chosen as the HER catalyst in this system because of its stability and solubility in low pH aqueous solvents.[25] An initial biomimetic study showed that molybdenum disulfide materials have the ability to catalyze efficiently the reduction of water.[26] Further studies have shown that molecular molybdenum sulfide catalysts, (e.g., $[Mo_3S_4]^{4+}$, $[Mo_3S_{13}]^{2-}$, and $[Mo_2S_{12}]^{2-}$) have an advantage over molybdenum disulfide 2D sheets for hydrogen evolution due to the increased number of active terminal sulfur sites.[27−29] The $[Mo_3S_4]^{4+}$ cluster has been shown to have HER activity similar to that of the edge site of 2D molybdenum disulfide sheets.[30−34] Therefore, it would be advantageous to incorporate such low-cost and active Mo_xS_y catalysts into DSPEC systems. However, Mo_xS_y clusters exhibit optimal activity in acidic environments.[28] Until now, using Mo_xS_y clusters in DSPECs has been unfeasible because photoelectrodes sensitized with dyes anchored to a metal oxide semiconductor have been unstable in even mildly acidic environments.[15]

EXPERIMENTAL METHODS

Synthesis. The $[Mo_3S_4(H_2O)_9]Cl_4$ cluster was synthesized according to prior literature.[34,35] The dye used, BH4, was synthesized according to our prior report.[19]

Film Preparation. The NiO films were prepared using a modified sol−gel method.[36−38] The green sol−gel solution was then doctor-bladed onto FTO glass and heated at 450 °C for 30 min. Film thickness was varied by repeated cycles of doctor-blading and heating. Film thickness was determined using an AlphaStep D-100 profilometer from KLA-Tencor Corporation. All films used were 0.8 ± 0.5 μm thick. NiO films were soaked overnight in 0.01 mM BH4 dye solution in DMF.

Buffer Preparation. Two separate 1 M solutions of citric acid (42.01 g) and sodium citrate (58.08 g) were prepared using 200 mL of deionized water (18 MΩ cm). To prepare the pH 3 and 5 buffers, 82 and 35 mL of the citric acid solution were added to two 100 mL Erlenmeyer flasks, respectively. A pH meter (Oakton, Ion 6 Acorn series) was calibrated (using pH 4 and 7 buffers from Fisher Scientific) and used to measure the pH as the citric acid solution was titrated with the sodium citrate solution until a pH of 3 (18.00 mL) and 5 (65.00 mL) were reached. The Erlenmeyer flasks were then fitted with septa and degassed for 1 h each by bubbling a strong flow of nitrogen through the solutions.

Cell Setup and Electrochemical Tests. The sensitized films were washed with DMF and air-dried before use. The photoelectrochemical measurements were acquired using our homemade cell, which consisted of a three-electrode setup all in the same compartment. The electrodes consisted of a working photocathode (described above), a platinum mesh counter electrode, and a saturated KCl Ag/AgCl reference electrode, which was calibrated with potassium ferricyanide. The assembled cell was degassed with nitrogen for 15−20 min prior to each experiment. All experiments contained 5 mM of catalyst. The photocathode electrode was illuminated with a 300 W xenon lamp fitted with a water jet filter and an additional filter to eliminate 420 nm wavelength light and avoid NiO light absorption. The light intensity was measured to be 344 mW/cm^2 using a Newport optical power meter (model 1830-C) equipped with a silicon diode detector (model 818-UV). Linear sweep voltammetry (LSV) was conducted at a scan rate of 2 mV/s with chopped light illumination in 20 s intervals for all LSV experiments. All CA experiments were held at a constant potential of 0 V vs NHE. The films' transmittance and electrolyte's absorbance prior to and after experiments were recorded using a PerkinElmer Lambda 950 instrument.

Hydrogen Detection. Hydrogen was detected using a Shimadzu gas chromatograph equipped with a thermal conductance detector using argon as the carrier gas. The instrument was calibrated by injecting known volumes of hydrogen.

DOI: 10.1021/jacs.5b07723
J. Am. Chem. Soc. 2016, 138, 1174−1179

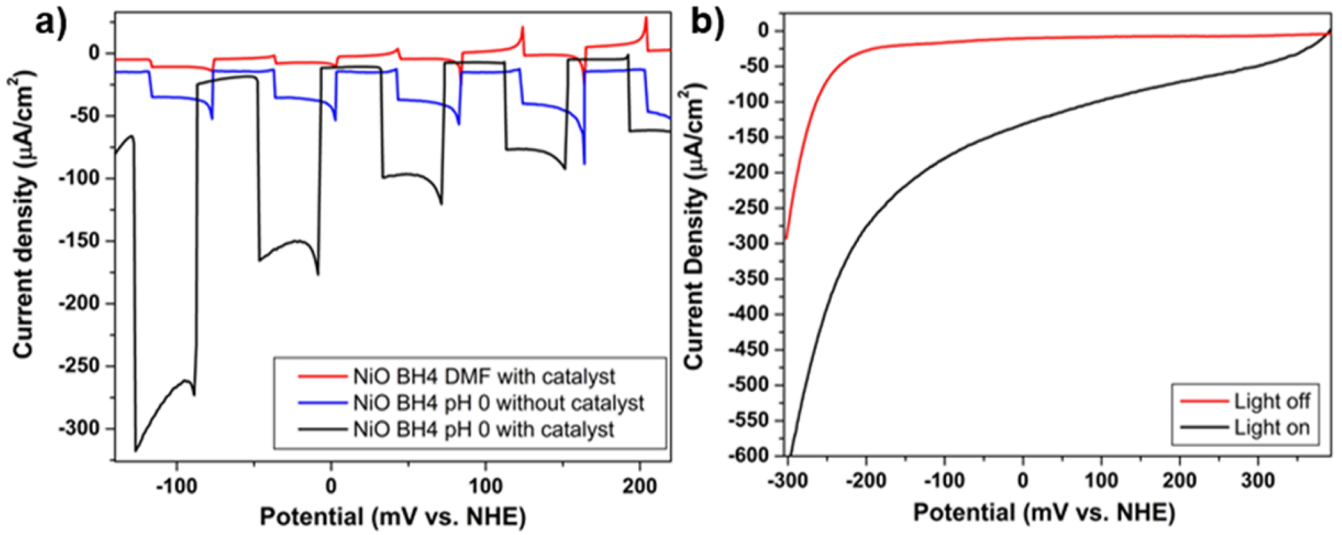

Figure 2. (a) Linear sweep voltammetry (LSV) scanning from 200 to −200 mV at a scan rate of 2 mV/s of all BH4-sensitized NiO films with varying electrolyte compositions, elucidating the requirement for catalyst, protons, dye, and light for current. (b) LSV scanning from 400 to −300 mV at 2 mV/s with light chopping of all BH4-sensitized NiO film in pH 0 (1 M HCl) electrolyte with 5 mM $[Mo_3S_4]^{4+}$ catalyst with light off (red trace) and light on (black trace).

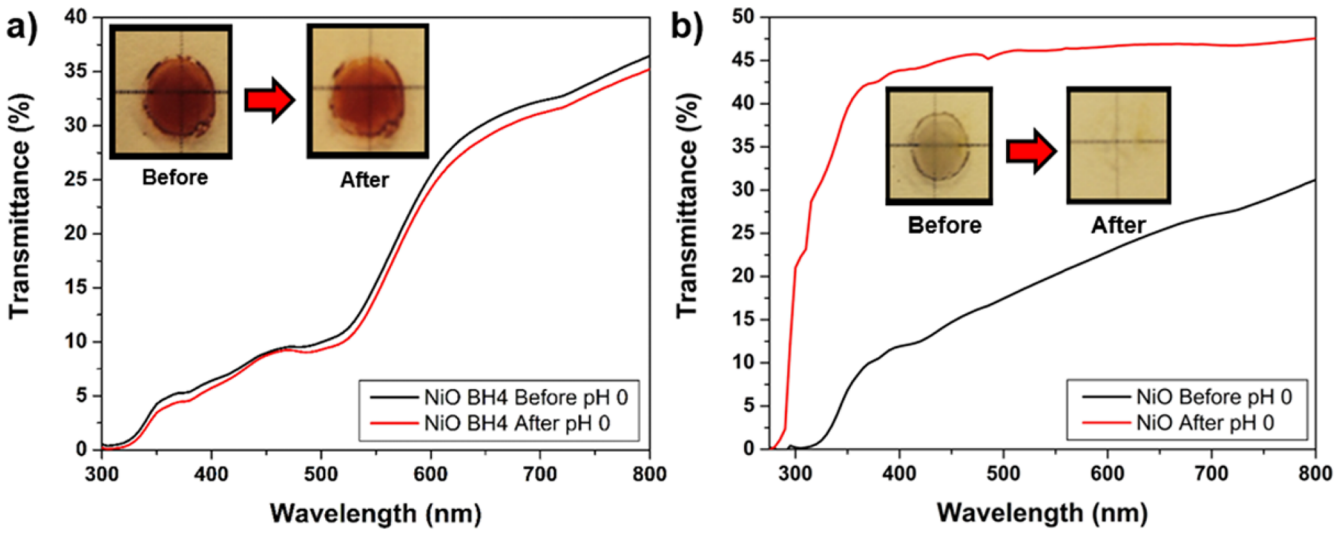

Figure 3. Transmittance of NiO films before and after a 3 h soak in 1 M HCl solution. (a) Transmittance of a BH4-sensitized NiO film before (black line) and after (red line) 3 h of soaking in a 1 M HCl (pH 0) solution showing no indication of degradation. Insets: BH4 film before (left) and after (right) soaking. (b) Transmittance of bare NiO films before (black line) and after (red line) a 3 h soak in 1 M HCl. Insets: Bare NiO film before (left) and after (right) soaking.

RESULTS AND DISCUSSION

The operating principle of the cell can be seen in Figure 1. Upon photoexciting the BH4 sensitizer, a hole is injected from the excited sensitizer into the valence band (VB) of NiO. The reduced dye then transfers an electron to $[Mo_3S_4]^{4+}$, after which the reduced $[Mo_3S_4]^{4+}$ can produce hydrogen from protons in the 1 M HCl electrolyte. BH4 has HOMO and LUMO positions of 1.64 and −0.64 V, respectively. NiO's VB has a position of 0.50 V.[19] The reduction potential of $[Mo_3S_4]^{4+}$ has been reported to be approximately −0.50 V at pH 0.[39] The energy alignment of all aspects of the DSPEC system are thermodynamically favorable, and the chronological sequence has been demonstrated by our group's previous studies.[14,40]

Control. To ensure that the system's light-response current can be attributed to hydrogen production, all variables were systematically probed. Three cells were built using BH4-sensitized nickel oxide (NiO) films and varying solvents and catalyst concentrations. The cells were evaluated via LSV, sweeping from 225 to −150 mV while light chopping. The first cell contained anhydrous dimethylformamide (DMF) and $[Mo_3S_4]^{4+}$ (Figure 2a). This aprotic system showed minimal light response, as did the system containing aqueous 1 M HCl solution without catalyst. When catalyst was added to the aqueous acidic system, a significant light response was observed. This shows that the light response is due to the presence of both a catalyst ($[Mo_3S_4]^{4+}$) and a proton source. LSV was conducted using a BH4-sensitized NiO film in a 1 M HCl (pH 0) electrolyte containing 5 mM of catalyst ($[Mo_3S_4]^{4+}$) scanning from 400 to −300 mV with light on and off (Figure 2b). LSV shows a large difference between the light and dark currents, confirming photoactivity of the system.

DOI: 10.1021/jacs.5b07723
J. Am. Chem. Soc. 2016, 138, 1174−1179

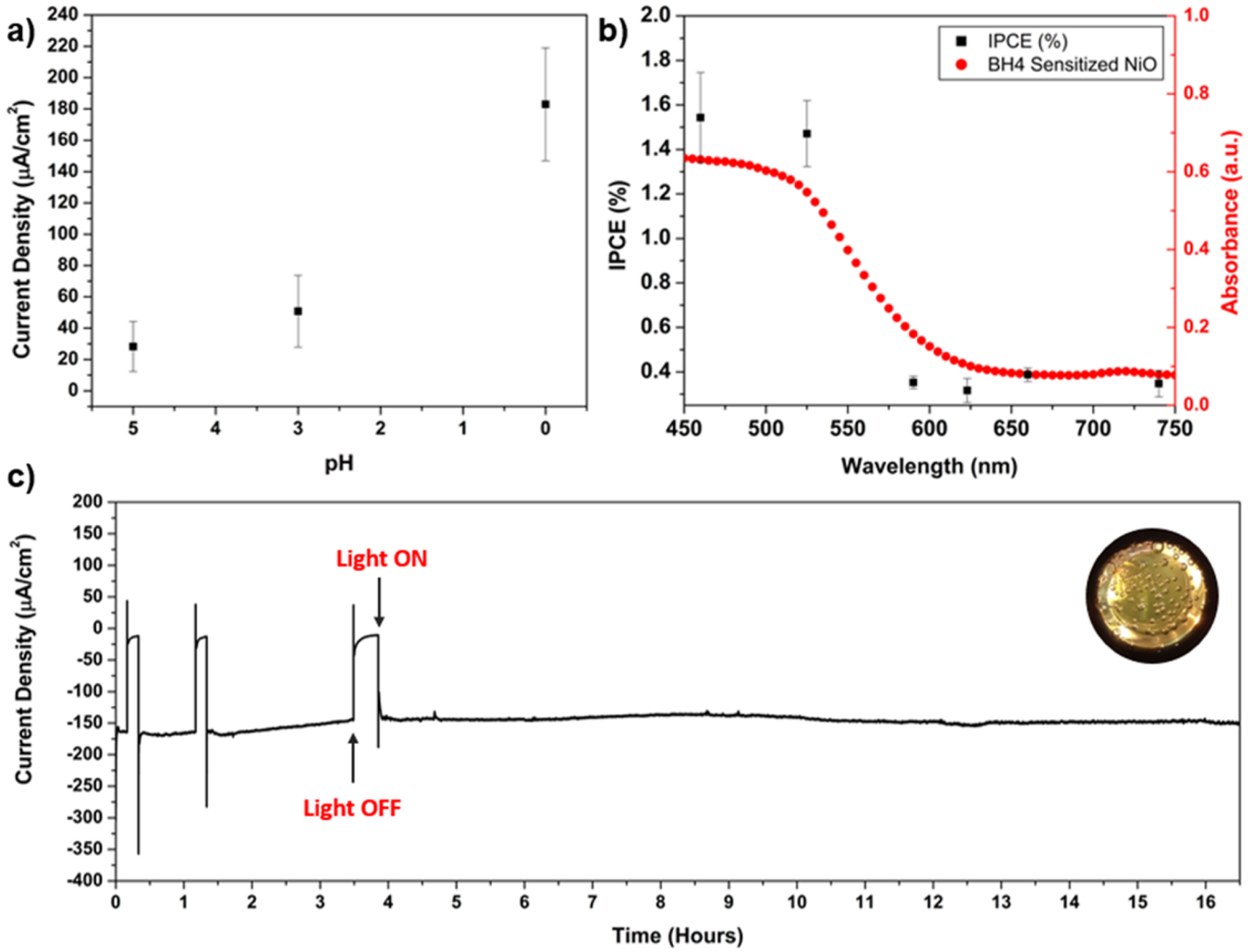

Figure 4. (a) Current densities of a BH4-sensitized NiO film in pH 5, 3, and 0 solutions, all containing 5 mM $[Mo_3S_4]^{4+}$ catalyst. (b) IPCE spectra of a pH 0 (1 M HCl) solution with 5 mM $[Mo_3S_4]^{4+}$ catalyst at an applied potential of −0.17 V (black squares) plotted with an absorbance spectra of a BH4-sensitized NiO film (red circles). (c) Chronoamperometry of a BH4-sensitized NiO film in pH 0 (1 M HCl) solution with 5 mM $[Mo_3S_4]^{4+}$ catalyst at an applied potential of 0 V with constant light illumination (aside from 3 light on/off tests). Inset: Hydrogen bubbles formed on the working electrode.

The onset for light current starts at 400 mV. Furthermore, the LSV shows that current densities of 300 μA/cm^2 can be obtained for the pH 0 solutions at a modest overpotential of −140 mV.

Stability under Strongly Acidic Conditions. To assess quantitatively the film stability, transmittance was carried out on a NiO film sensitized with BH4 and a control film of bare NiO (without BH4 dye protection). The transmittances of the films were evaluated before and after 3 h of exposure to the 1 M HCl electrolyte, which can be seen in Figure 3 (pH 5 and 3, Figures S1 and S2, respectively). The transmittance of the film with the BH4 dye shows no change, indicating that no dye desorption or film degradation occurred. The bare NiO film without the BH4 dye protection showed a dramatic change in transmittance as well as a change in the visible appearance (Figure 3b inset), indicating that the NiO film dissolved into the acidic electrolyte. To quantify further the stability of the photocathode, both nonsensitized and BH4-sensitized NiO films were soaked in separate pH 0 (1 M HCl) solutions for 3 h each; then, the solutions were analyzed via inductively coupled plasma optical emission spectroscopy (ICP-OES). The bare NiO film without BH4 protection showed 2.3 ppm of Ni^{2+} in the solution, whereas both the BH4-sensitized NiO film and the control solution (1 M HCl) showed less than 0.35 ppm of Ni^{2+} (Table S1 and Figure S3 for pH 3). These results show that the dual-function BH4 dye sufficiently protects the surface of NiO from both acid dissolution and dye desorption, as evidenced by the cell's remarkable 16.6 h of continuous performance shown later. Further evidence of the NiO protection afforded by BH4's canopy of lipophilic hexyl groups is demonstrated by contact angle comparison of a pH 0 droplet: 119° for the BH4-sensitized film compared to 12° for the bare NiO (Figure S4). Such high acidic stability is unprecedented. To the best of our knowledge, only one qualitative study has shown photocathode stability under acidic conditions using a PMI-6T-TPA sensitizer anchored on NiO as the photosensitizer.[13] However, no catalyst was employed in that study, nor was the cathode operated under acidic conditions.[41]

Effect of pH on Photocurrent. The only two tandem DSPECs demonstrated to date, by Sun et al., were constrained to pH 7 and showed notable photocurrent decay in that only ∼60% of the photocurrent remained after the first 10 min of illumination.[3,4] The photoanode in these systems could produce an average photocurrent of 300 μA/cm^2 (0 V vs

DOI: 10.1021/jacs.5b07723
J. Am. Chem. Soc. 2016, 138, 1174−1179

Ag/AgCl), whereas the photocathode only produced an average photocurrent of 35 μA/cm^2 (−0.2 V vs Ag/AgCl) with both illuminated by 100 mW/cm^2 light. Hence, the photocathode limited the tandem DSPEC. Additionally, the stability of all p-type DSPEC systems has been limited to pH 7.[13−16] It would be advantageous to increase the stability of these systems not only in pH 7 but also over a range of pH values. The system reported here shows long-term stability in pH 5, 3, and 0 solutions under visible light irradiation. The influence of the system's pH was tested via CA with an applied potential of 0 V for pH 0, 3, and 5 (Figure 4a) and LSV (Figures S5 and S6, respectively). As the hydronium concentration is increased, the light-induced current also increases.

One would expect current to increase at lower pH values because of increased kinetics for hydrogen production. This contradicts the results recently obtained by Castillo et al.[15] They observed a decrease in current as the pH decreased, which was explained by NiO's flat band potential becoming more positive with increased proton concentration at the NiO surface, thus decreasing hole-injection driving force. Indeed, Grätzel et al., O'Regan et al., and others have shown that as positive charge accumulates on the surface of a dye-sensitized solar cell's (DSSCs) metal oxide semiconductor the band edge of the semiconductor shifts to more positive values.[15,42−45] In our case, this effect would also decrease the driving force for hole injection from the dye's HOMO to the semiconductor's valence band. However, we have observed that at lower pH values light-induced current increases significantly suggesting that positive charge is not accumulating at the NiO surface. This can be explained by the shielding of the NiO semiconductor from hydronium ions by BH4's inherent steric bulk and amphiphilic character, which is supported by the ICP results previously mentioned. This concept has been proven by Grätzel et al. and O'Reagan et al.[46−49] to increase the stability and performance of closely related DSSCs in both organic and aqueous electrolytes, which has been summarized in a review.[50] Surprisingly, to date this strategy has not been employed for DSPECs. Additionally, it is known that metal oxides can be dissolved by acidic solutions, yet this was not observed for our BH4-sensitized NiO films, further supporting the utility of this strategy.[51]

Efficiency. Incident to photon current efficiency (IPCE) was determined for a BH4-sensitized NiO film with 5 mM catalyst in pH 0 at an applied potential (−0.17 V vs NHE) where the light response was the largest (Figure 4b). The IPCE spectrum closely matches the BH4-sensitized NiO film absorbance spectrum (Figure 4b, red circles), confirming that the current is due to light absorption from the dye. Gas chromatography coupled to a thermal conductance detector (GC-TCD) was employed to verify the evolution of hydrogen from a cell with 5 mM catalyst in pH 0 with an applied potential of −0.3 V. After irradiation, GC-TCD was used to measure the hydrogen present in 1.0 mL aliquots taken from the head space of the cell (6.5 mL). A faradic efficiency up to 60% was calculated with an average of 49 ± 11% over 5 experiments. The faradic efficiency can be attributed to the irreversibility of the Mo^{4+} reduction, which has been observed in prior HER studies using this cluster.[30,52,53] UV−vis spectrometry of the electrolyte solution (5 mM $[Mo_3S_4]^{4+}$ in pH 0, 1 M HCl) before and after CA held for 2.7 h with constant light illumination shows a change in the UV−vis spectra of the $[Mo_3S_4]^{4+}$ cluster, signifying decomposition of the catalyst (Figure S8). However, no change in the films transmittance was observed after photoelectrolysis (Figure S9), indicating no deposition of any Mo_xS_y species onto the photocathode. However, CA experiments show stable current over 16.6 h despite the faradaic efficiency.

Long-Term Operating Stability. CA (Figure 2c) was then conducted at 0 V at pH 0 with 5 mM catalyst, and the current response was measured as a function of time. The light was allowed to irradiate the film continuously for 16.6 h apart from three brief light-on and -off periods to confirm that the current could still be attributed to the light. The cell shows stable currents (183 ± 36 μA/cm^2) over this time period. This length of stable performance has never been shown before for any DSPEC, either n- or p-type, and was carried out in an environment much more acidic than that of previous studies (1 M HCl).

CONCLUSIONS

This study demonstrates the first acidically stable dye-sensitized photocathode as well as incorporating a non-noble-metal cluster as a catalyst for water reduction. The current densities (183 ± 36 μA/cm^2 and as high as 254 μA/cm^2) obtained at an applied bias of 0 and −0.2 V, respectively, with a 300W Xe lamp source are the highest current densities obtained for p-type DSPECs at any applied potential. The 16.6 h of photocathode stability in 1 M HCl is unprecedented. Additionally, we have shown that a primary reason for the decreased performance and instability of NiO-based (and likely other metal oxide semiconductor based) DSPEC systems in acidic environments is the dye desorption and/or dissolution of the metal oxide. Therefore, we suggest using bulky hydrophobic sensitizers such as BH4 to protect the metal oxide semiconductor and improve dye-sensitized photocathode stability, especially under extremely acidic conditions. This advancement not only allows for more-efficient, low-pH water-reduction DSPECs but also moves dye-sensitized systems closer to practical applications by developing a method for protecting the semiconductor surface and using dye-sensitized photocathodes in any system that requires low pH.

ASSOCIATED CONTENT

Supporting Information

The Supporting Information is available free of charge on the ACS Publications website at DOI: 10.1021/jacs.5b07723.

Transmittance data for BH4 NiO film; transmittance data for BH4 NiO film before and after photoelectrolysis; UV−vis data of $[Mo_3S_4]^{4+}$ cluster and $[(Mo_3S_4)(H_2O)_9]Cl_4$; density data of BH4-sensitized film; ICPE calculation method, data, and spectra; and chronoamperometry at varying pH and linear sweep voltametry at varying pH with and without light chopping of $[Mo_3S_4]^{4+}$. For bare and BH4-sensitized films: ICP-OES data, photos of films before and after soaking in pH 3 solution, and contact angle data. (PDF)

AUTHOR INFORMATION

Corresponding Author

*E-mail: wu@chemistry.ohio-state.edu. Fax: +1-614-292-1685. Tel.: +1-614-247-7810.

Notes

The authors declare no competing financial interest.

DOI: 10.1021/jacs.5b07723
J. Am. Chem. Soc. 2016, 138, 1174−1179

■ ACKNOWLEDGMENTS

We acknowledge the funding support from the U.S. Department of Energy (Award No. DE-FG02−07ER46427).We thank Dr. Turro and Suzanne Witt for the use of their GC-TCD; Ben Garrett, Billy McCulloch, and Tom Draskovic for fruitful conversations; and Trace Element Research Laboratory (TERL) and Anthony Lutton for ICP-OES sample analysis.

■ REFERENCES

(1) Song, W.; Chen, Z.; Glasson, C. R. K.; Hanson, K.; Luo, H.; Norris, M. R.; Ashford, D. L.; Concepcion, J. J.; Brennaman, M. K.; Meyer, T. J. *ChemPhysChem* **2012**, *13*, 2882−2890.
(2) Youngblood, W. J.; Lee, S.-H. A.; Maeda, K.; Mallouk, T. E. *Acc. Chem. Res.* **2009**, *42*, 1966−1973.
(3) Fan, K.; Li, F.; Wang, L.; Daniel, Q.; Gabrielsson, E.; Sun, L. *Phys. Chem. Chem. Phys.* **2014**, *16*, 25234−25240.
(4) Li, F.; Fan, K.; Xu, B.; Gabrielsson, E.; Daniel, Q.; Li, L.; Sun, L. *J. Am. Chem. Soc.* **2015**, *137*, 9153−9159.
(5) Swierk, J. R.; Mallouk, T. E. *Chem. Soc. Rev.* **2013**, *42*, 2357−2387.
(6) Zhao, Y.; Swierk, J. R.; Megiatto, J. D.; Sherman, B.; Youngblood, W. J.; Qin, D.; Lentz, D. M.; Moore, A. L.; Moore, T. A.; Gust, D.; Mallouk, T. E. *Proc. Natl. Acad. Sci. U. S. A.* **2012**, *109*, 15612−15616.
(7) Youngblood, W. J.; Lee, S.-H. A.; Kobayashi, Y.; Hernandez-Pagan, E. A.; Hoertz, P. G.; Moore, T. A.; Moore, A. L.; Gust, D.; Mallouk, T. E. *J. Am. Chem. Soc.* **2009**, *131*, 926−927.
(8) Concepcion, J. J.; House, R. L.; Papanikolas, J. M.; Meyer, T. J. *Proc. Natl. Acad. Sci. U. S. A.* **2012**, *109*, 15560−15564.
(9) Alibabaei, L.; Brennaman, M. K.; Norris, M. R.; Kalanyan, B.; Song, W.; Losego, M. D.; Concepcion, J. J.; Binstead, R. A.; Parsons, G. N.; Meyer, T. J. *Proc. Natl. Acad. Sci. U. S. A.* **2013**, *110*, 20008−20013.
(10) Brimblecombe, R.; Koo, A.; Dismukes, G. C.; Swiegers, G. F.; Spiccia, L. *J. Am. Chem. Soc.* **2010**, *132*, 2892−2894.
(11) Gao, Y.; Ding, X.; Liu, J.; Wang, L.; Lu, Z.; Li, L.; Sun, L. *J. Am. Chem. Soc.* **2013**, *135*, 4219−4222.
(12) Ding, X.; Gao, Y.; Zhang, L.; Yu, Z.; Liu, J.; Sun, L. *ACS Catal.* **2014**, *4*, 2347−2350.
(13) Tong, L.; Iwase, A.; Nattestad, A.; Bach, U.; Weidelener, M.; Götz, G.; Mishra, A.; Bäuerle, P.; Amal, R.; Wallace, G. G.; Mozer, A. J. *Energy Environ. Sci.* **2012**, *5*, 9472.
(14) Ji, Z.; He, M.; Huang, Z.; Ozkan, U.; Wu, Y. *J. Am. Chem. Soc.* **2013**, *135*, 11696−11699.
(15) Castillo, C. E.; Gennari, M.; Stoll, T.; Fortage, J.; Deronzier, A.; Collomb, M.-N.; Sandroni, M.; Légalité, F.; Blart, E.; Pellegrin, Y.; Delacote, C.; Boujtita, M.; Odobel, F.; Rannou, P.; Sadki, S. *J. Phys. Chem. C* **2015**, *119*, 5806−5818.
(16) Li, L.; Duan, L.; Wen, F.; Li, C.; Wang, M.; Hagfeldt, A.; Sun, L. *Chem. Commun.* **2012**, *48*, 988.
(17) Yu, Z.; Li, F.; Sun, L. *Energy Environ. Sci.* **2015**, *8*, 760−775.
(18) Concepcion, J. J.; Jurss, J. W.; Hoertz, P. G.; Meyer, T. J. *Angew. Chem., Int. Ed.* **2009**, *48*, 9473−9476.
(19) Click, K. A.; Beauchamp, D. R.; Garrett, B. R.; Huang, Z.; Hadad, C. M.; Wu, Y. *Phys. Chem. Chem. Phys.* **2014**, *16*, 26103−26111.
(20) Raven, P. H.; Evert, R. F.; Eichhorn, S. E. *Biology of Plants*, 7th ed.; W. H. Freeman, 2005; pp 115−127.
(21) Ji, Z.; Natu, G.; Huang, Z.; Kokhan, O.; Zhang, X.; Wu, Y. *J. Phys. Chem. C* **2012**, *116*, 16854−16863.
(22) Nattestad, A.; Mozer, A. J.; Fischer, M. K. R.; Cheng, Y.-B.; Mishra, A.; Bäuerle, P.; Bach, U. *Nat. Mater.* **2010**, *9*, 31−35.
(23) Kroeze, J. E.; Hirata, N.; Koops, S.; Nazeeruddin, M. K.; Schmidt-Mende, L.; Grätzel, M.; Durrant, J. R. *J. Am. Chem. Soc.* **2006**, *128*, 16376−16383.
(24) Jacques, P.-A.; Artero, V.; Pécaut, J.; Fontecave, M. *Proc. Natl. Acad. Sci. U. S. A.* **2009**, *106*, 20627−20632.
(25) Saysell, D. M.; Sykes, A. G. *J. Cluster Sci.* **1995**, *6*, 449−461.
(26) Hinnemann, B.; Moses, P. G.; Bonde, J.; Jørgensen, K. P.; Nielsen, J. H.; Horch, S.; Chorkendorff, I.; Nørskov, J. K. *J. Am. Chem. Soc.* **2005**, *127*, 5308−5309.
(27) Karunadasa, H. I.; Montalvo, E.; Sun, Y.; Majda, M.; Long, J. R.; Chang, C. J. *Science (Washington, DC, U. S.)* **2012**, *335*, 698−702.
(28) Kibsgaard, J.; Jaramillo, T. F.; Besenbacher, F. *Nat. Chem.* **2014**, *6*, 248−253.
(29) Huang, Z.; Luo, W.; Ma, L.; Yu, M.; Ren, X.; He, M.; Polen, S.; Click, K.; Garrett, B.; Lu, J.; Amine, K.; Hadad, C.; Chen, W.; Asthagiri, A.; Wu, Y. *Angew. Chem., Int. Ed.* **2015**, *54*, 15181−15185.
(30) Jaramillo, T. F.; Bonde, J.; Zhang, J.; Ooi, B.-L.; Andersson, K.; Ulstrup, J.; Chorkendorff, I. *J. Phys. Chem. C* **2008**, *112*, 17492−17498.
(31) Hernandez-Molina, R.; Sokolov, M. N.; Sykes, A. G. *Acc. Chem. Res.* **2001**, *34*, 223−230.
(32) Hou, Y.; Abrams, B. L.; Vesborg, P. C. K.; Björketun, M. E.; Herbst, K.; Bech, L.; Setti, A. M.; Damsgaard, C. D.; Pedersen, T.; Hansen, O.; Rossmeisl, J.; Dahl, S.; Nørskov, J. K.; Chorkendorff, I. *Nat. Mater.* **2011**, *10*, 434−438.
(33) Coucouvanis, D. Solid-State Materials and Clusters. In *Inorganic Syntheses*; Wiley: New York, 2002; Vol. *33*, pp 112.
(34) Martinez, M.; Ooi, B. L.; Sykes, A. G. *J. Am. Chem. Soc.* **1987**, *109*, 4615−4619.
(35) Sakane, G., Shibahara, T. In *Solid-State Materials and Clusters*; Wiley: New York, 2002; Vol. 33; pp 144, 150
(36) Sumikura, S.; Mori, S.; Shimizu, S.; Usami, H.; Suzuki, E. *J. Photochem. Photobiol., A* **2008**, *199*, 1−7.
(37) Li, L.; Gibson, E. A.; Qin, P.; Boschloo, G.; Gorlov, M.; Hagfeldt, A.; Sun, L. *Adv. Mater.* **2010**, *22*, 1759−1762.
(38) He, M.; Ji, Z.; Huang, Z.; Wu, Y. *J. Phys. Chem. C* **2014**, *118*, 16518−16525.
(39) Seo, S. W.; Park, S.; Jeong, H.-Y.; Kim, S. H.; Sim, U.; Lee, C. W.; Nam, K. T.; Hong, K. S. *Chem. Commun. (Cambridge, U. K.)* **2012**, *48*, 10452−10454.
(40) Ji, Z.; Natu, G.; Huang, Z.; Kokhan, O.; Zhang, X.; Wu, Y. *J. Phys. Chem. C* **2012**, *116*, 16854−16863.
(41) Tong, L.; Iwase, A.; Nattestad, A.; Bach, U.; Weidelener, M.; Götz, G.; Mishra, A.; Bäuerle, P.; Amal, R.; Wallace, G. G.; Mozer, A. J. *Energy Environ. Sci.* **2012**, *5*, 9472.
(42) Gregg, B. A.; Chen, S.-G.; Ferrere, S. *J. Phys. Chem. B* **2003**, *107*, 3019−3029.
(43) Wang, Q.; Zhang, Z.; Zakeeruddin, S. M.; Gratzel, M. *J. Phys. Chem. C* **2008**, *112*, 7084−7092.
(44) Listorti, A.; Creager, C.; Sommeling, P.; Kroon, J.; Palomares, E.; Fornelli, A.; Breen, B.; Barnes, P. R. F.; Durrant, J. R.; Law, C.; O'Regan, B. *Energy Environ. Sci.* **2011**, *4*, 3494.
(45) Yang, L.; Xu, B.; Bi, D.; Tian, H.; Boschloo, G.; Sun, L.; Hagfeldt, A.; Johansson, E. M. J. *J. Am. Chem. Soc.* **2013**, *135*, 7378−7385.
(46) Nazeeruddin, M. K.; Zakeeruddin, S. M.; Lagref, J.-J.; Liska, P.; Comte, P.; Barolo, C.; Viscardi, G.; Schenk, K.; Graetzel, M. *Coord. Chem. Rev.* **2004**, *248*, 1317−1328.
(47) Wang, P.; Zakeeruddin, S. M.; Moser, J. E.; Nazeeruddin, M. K.; Sekiguchi, T.; Grätzel, M. *Nat. Mater.* **2003**, *2*, 402−407.
(48) Law, C.; Moudam, O.; Villarroya-Lidon, S.; O'Regan, B. *J. Mater. Chem.* **2012**, *22*, 23387.
(49) Law, C.; Pathirana, S. C.; Li, X.; Anderson, A. Y.; Barnes, P. R. F.; Listorti, A.; Ghaddar, T. H.; O'Regan, B. C. *Adv. Mater.* **2010**, *22*, 4505−4509.
(50) Asghar, M. I.; Miettunen, K.; Halme, J.; Vahermaa, P.; Toivola, M.; Aitola, K.; Lund, P. *Energy Environ. Sci.* **2010**, *3*, 418.
(51) Valverde, N. *Berichte der Bunsengesellschaft für Phys. Chemie* **1976**, *80*, 333−340.
(52) Zhang, W.; Zhou, T.; Zheng, J.; Hong, J.; Pan, Y.; Xu, R. *ChemSusChem* **2015**, *8*, 1464−1471.
(53) Yan, Y.; Xia, B.; Xu, Z.; Wang, X. *ACS Catal.* **2014**, *4*, 1693−1705.

DOI: 10.1021/jacs.5b07723
J. Am. Chem. Soc. 2016, 138, 1174−1179